Osteoporosis International (2018) 29:685–697
https://doi.org/10.1007/s00198-017-4323-6

ORIGINAL ARTICLE

Abaloparatide, a novel PTH receptor agonist, increased bone mass and strength in ovariectomized cynomolgus monkeys by increasing bone formation without increasing bone resorption

N. Doyle[1] · A. Varela[1] · S. Haile[1] · R. Guldberg[2] · P. J. Kostenuik[3,4] · M. S. Ominsky[5] · S. Y. Smith[1] · G. Hattersley[5]

Received: 1 June 2017 / Accepted: 20 November 2017 / Published online: 19 December 2017

Abstract

Summary Abaloparatide, a novel PTH1 receptor agonist, increased bone formation in osteopenic ovariectomized cynomolgus monkeys while increasing cortical and trabecular bone mass. Abaloparatide increased bone strength and maintained or enhanced bone mass-strength relationships, indicating preserved or improved bone quality.

Introduction Abaloparatide is a selective PTH1R activator that is approved for the treatment of postmenopausal osteoporosis. The effects of 16 months of abaloparatide administration on bone formation, resorption, density, and strength were assessed in adult ovariectomized (OVX) cynomolgus monkeys (cynos).

Methods Sixty-five 9–18-year-old female cynos underwent OVX surgery, and 15 similar cynos underwent sham surgery. After a 9-month period without treatments, OVX cynos were allocated to four groups that received 16 months of daily s.c. injections with either vehicle ($n = 17$) or abaloparatide (0.2, 1, or 5 μg/kg/day; $n = 16$/dose level), while Sham controls received s.c. vehicle ($n = 15$). Bone densitometry (DXA, pQCT, micro-CT), qualitative bone histology, serum calcium, bone turnover markers, bone histomorphometry, and bone strength were among the key measures assessed.

Results At the end of the 9-month post-surgical bone depletion period, just prior to the treatment phase, the OVX groups exhibited increased bone turnover markers and decreased bone mass compared with sham controls. Abaloparatide administration to OVX cynos led to increased bone formation parameters, including serum P1NP and endocortical bone formation rate. Abaloparatide administration did not influence serum calcium levels, bone resorption markers, cortical porosity, or eroded surfaces. Abaloparatide increased bone mass at the whole body, lumbar spine, tibial diaphysis, femoral neck, and femoral trochanter. Abaloparatide administration was associated with greater lumbar vertebral strength, and had no adverse effects on bone mass-strength relationships for the vertebrae, femoral neck, femoral diaphysis, or humeral cortical beams.

Conclusions Abaloparatide administration was associated with increases in bone formation, bone mass and bone strength, and with maintenance of bone quality in OVX cynos, without increases in serum calcium or bone resorption parameters.

Keywords Abaloparatide · Bone quality · Bone strength · Osteoporosis · PTH1R

Parts of these studies were presented previously at the ASBMR's 36th Annual meeting, September 12–15, 2014, Houston TX, and at the Endocrine Society's 97th Annual Meeting, March 5–8, 2015, San Diego, CA.

Electronic supplementary material The online version of this article (https://doi.org/10.1007/s00198-017-4323-6) contains supplementary material, which is available to authorized users.

✉ G. Hattersley
ghattersley@radiuspharm.com

[1] Charles River Laboratories, Montreal, QC, Canada

[2] School of Mechanical Engineering, Georgia Institute of Technology, Atlanta, GA, USA

[3] University of Michigan, Ann Arbor, MI, USA

[4] Phylon Pharma Services, Newbury Park, CA, USA

[5] Radius Health Inc., 950 Winter Street, Waltham, MA 02451, USA

Introduction

Abaloparatide is a novel PTH1R agonist with 41% homology to PTH(1–34) (teriparatide) and 76% homology to PTHrP. Abaloparatide was selected for its potential to stimulate bone formation with limited effects on bone resorption or serum calcium [1]. Clinical trials in postmenopausal women with osteoporosis showed that abaloparatide significantly increased bone mineral density (BMD) at the lumbar spine, hip, and femoral neck and reduced the risk of vertebral, nonvertebral, major osteoporotic, and clinical fractures [2, 3].

A study in osteopenic ovariectomized (OVX) rats showed that 12 months of abaloparatide administration increased bone formation on trabecular, endocortical, and periosteal surfaces without increasing histologic or biochemical indices of bone resorption [4]. These effects were accompanied by significant gains in bone mass and strength of lumbar vertebra, the femoral diaphysis, and femoral neck relative to vehicle (Veh) controls [5]. There was no evidence from OVX rats for adverse effects of abaloparatide on bone quality, defined as structural and material properties of bone that determine its biomechanical behavior in ways not accounted for by bone mass [6]. However, unlike humans, OVX rats lack physiological remodeling within cortical bone, so larger species with intracortical remodeling are important for bone safety assessments. Species with intracortical remodeling are particularly relevant for assessing PTH1R activators because their intermittent administration often increases intracortical remodeling, which can increase cortical porosity [7–11] and reduce cortical BMD [9–13].

Cynomolgus monkeys (cynos) exhibit physiological intracortical, endocortical, and trabecular remodeling that is increased by ovariectomy-induced estrogen deficiency, typically leading to reductions in trabecular and cortical bone mass and decreased bone strength [14, 15]. Ovariectomized (OVX) cynos are a commonly used large animal model for assessing the safety, efficacy, and mechanism of action of osteoporosis medications [14]. Previous cyno studies with up to 10 months of treatment showed that abaloparatide administration was associated with BMD gains and increased bone formation by histomorphometry, without changes in blood calcium levels or histomorphometric parameters of bone resorption [16–18]. The current 16-month treatment study was conducted in osteopenic OVX cynos to understand the longer-term effects of abaloparatide on these and other endpoints, including bone turnover markers, bone strength, and bone material properties that reflect bone quality.

Materials and methods

Animals and study design

All animal-related activities were approved by the Charles River Montreal's Animal Care Committee and performed in an AAALAC-accredited facility. The study was performed under Good Laboratory Practice (GLP) in accordance with the protocol and standard operating procedures at Charles River Laboratories.

Eighty-four female cynos from Mauritius, including spare animals, were received from Primus Bio Resources, aged 9 to 18 years and weighing 3.1 to 6.9 kg. Animals were housed 2–3/stainless steel cage (temperature range 21–27 °C, humidity 30–70%, 12–12-h light-dark cycle), in conformance with accepted AAALAC requirements. Animals had access to standard 2056 Teklad Certified Global Soy-Protein-Free food pellets (Harlan Teklad) and automated watering valves.

A 5-week acclimation period included detailed health exams, including menstrual regularity and body weight. After acclimation, animals underwent DXA scanning. Age, body weight, whole body bone mineral content (BMC), and lumbar spine BMD guided allocation into five treatment groups ($n = 15$–17/group). Four groups underwent OVX while the fifth group underwent sham surgery, as previously described [15]. After surgery, animals remained untreated for 9 months to allow OVX-induced bone loss. Sham controls and one OVX group then received daily s.c. vehicle (0.9% saline; Sham, $n = 15$; Veh, $n = 17$) for 16 months, while other OVX groups received daily s.c. abaloparatide at 0.2, 1, or 5 μg/kg (ABL0.2, ABL1, and ABL5; all $n = 16$). Dose selection was guided by BMD data from a previous 10-month cyno study, which showed reversal of OVX-induced BMD loss with abaloparatide at 1 and 10 μg/kg/day [17]. Therefore, 1 μg/kg was designated as the pharmacologically effective dose in this species; a fivefold lower dose (0.2 μg/kg) was included as a "suboptimal" dose, and a fivefold higher dose (5 μg/kg) was included to provide an adequate safety margin, in accordance with regulatory guidelines [19, 20].

Regular animal monitoring included food consumption and menstrual status. Detailed weekly clinical evaluations included body weight. At the end of the treatment period, overnight-fasted animals were sedated with i.m. ketamine (15 mg/kg), anesthetized with a weight-based volume of sodium pentobarbital, and euthanized by exsanguination. Gross examinations and full necropsies were performed and internal organs weighed.

Histopathology and radiography

Major organs and numerous other tissues were collected at necropsy and evaluated for gross changes. All collected samples were evaluated microscopically for pathologic changes if they exhibited gross changes, and some samples underwent prospective microscopic evaluations, including distal femurs, sternum, 10th thoracic vertebra, heart, kidney, lung, ovary, and uterus.

Dorso-ventral and lateral radiographs of the lumbar and thoracic spine and appendicular long bones (including hip) were taken at the beginning and end of the treatment period and examined for skeletal abnormalities, including any suspected focal proliferative changes that developed or progressed compared with pre-treatment evaluation. Radiographic lesions were collected at scheduled euthanasia, decalcified, and examined microscopically.

Clinical chemistry and bone turnover markers

Blood was collected by femoral venipuncture after overnight fasting for clinical chemistry (serum calcium, phosphorus, and creatinine; 0.7 mL of blood collected into serum separator tubes) and for bone turnover markers estradiol, PTH(1–84), and $1,25(OH)_2D$ (6 mL of blood collected into serum separator tubes). Morning urine was collected by catheterization after anesthesia with i.m. glycopyrrolate (0.01 mg/kg), ketamine (5 or 10 mg/kg), xylazine (0.6 mg/kg), or dexmedetomidine (0.01 mg/kg). Serum procollagen 1 N-terminal peptide (P1NP) was measured by UniQ P1NP RIA kits from Orion Diagnostica (Cat. no. 67034), serum bone-specific alkaline phosphatase (BSAP) by MicroVue™ BAP EIA kits from Quidel Corp. (Cat. no. 8012), and serum C-telopeptides (CTX) by Serum CrossLaps ELISA kits (IDS Inc., Cat. no. AC-02F1). Urine N-telopeptides (NTX) was measured by Osteomark NTx Urine ELISA kits (Wampole Laboratories, Cat. no. WL-9006) and adjusted for urine creatinine. Additional serum analyses included estradiol (Ultra-Sensitive Estradiol RIA kit, Beckman Coulter, no. DSL4800), $1,25(OH)_2D$ (RIA kit, IDS Ltd., no. AA54F2), and PTH(1–84) (human PTH ELISA kit, Immutopics, Inc., no. 60-3100).

Bone histomorphometry

Fifteen and 5 days prior to month 16 sacrifice, animals received i.v. bicarbonate-buffered calcein (8 mg/kg). At necropsy, the second lumbar vertebra (L2) and left femur (neck and mid-shaft) were trimmed with a diamond saw and stored in 10% formalin for 3 days. Samples were transferred to 70% ethanol and prepared undecalcified. Tissue blocks were cut through the median plane of the L2 vertebral body and transversely at the left femoral mid-shaft, and the femoral neck was trimmed along the frontal plane. Blocks were dehydrated in ethanol and embedded in methylmethacrylate. Unstained sections from trabecular bone regions were cut at 4–8 μm thickness with a Leica RM2255 rotary microtome and mounted on microscope slides. Unstained sections from cortical bone regions were ground (40–80 μm thick) on an Exakt 400CS micro-grinder and mounted on microscope slides, with two section levels evaluated at the middle of the femoral diaphysis. Trabecular analyses were performed on unstained sections (7 μm) and on sections stained with toluidine blue and Goldner's trichrome (5 μm). Histomorphometry data were generated by ImagePro Plus® using standard methods and nomenclature [21]. Evaluation of the cancellous bone region was done on the femoral neck (two section levels) and L2 (one section level). Cancellous bone measurements were confined within predetermined lines traced on sections and excluded an approximately 0.25-mm-wide transitional zone between the cancellous and cortical bone tissue. The area of interest (AOI) in L2 comprised two 16-mm^2 squares traced at each end of the vertebral body, centered through the dorso-ventral plane and starting at 1 mm from the inner edge of the physis. The AOI measured in the proximal femur comprised a 16-mm^2 square traced in the proximal to mid-femoral neck. Evaluation of cortical bone was performed on two levels of the whole section.

Whenever the mineral apposition rate (MAR) could not be directly measured in a specific bone region of an individual animal due to lack of double fluorochrome labels, a value of 0.2 μm/day was used for MAR of that region in that animal, representing the smallest measurable inter-label distance. For trabecular analyses, the femoral neck of one vehicle control animal exhibited no double label; for cortical analyses, details on labeling status are provided in Section 3.

Bone densitometry

In vivo DXA was performed with a Hologic Discovery A densitometer; sites and analysis modes included whole body (infant whole body analysis mode), lumbar spine (L1-L4), proximal tibial diaphysis, and right proximal femur (neck plus trochanter, subregion array spine analysis mode). Before each scan, animals were anesthetized by i.m. glycopyrrolate (0.01 mg/kg), ketamine (5 or 10 mg/kg), xylazine (0.6 mg/kg), or dexmedetomidine (0.01 mg/kg). Ex vivo (month 16) DXA scans were obtained for the right femur (total, proximal, central, and distal), L3 and L4 bodies, and L5 and L6 cancellous cores.

In vivo pQCT scans were performed with an XCT Research SA+ bone scanner, software version 5.50. Three sequential scans, 0.5 mm apart, were obtained at the proximal tibia and distal radial metaphysis, with an additional slice in each bone's diaphysis. The metaphyseal region included total, trabecular, and cortical/subcortical compartments, the latter representing total minus trabecular, while the diaphyseal region comprised cortical bone only. An XCT Research SA bone scanner was used for ex vivo assessments of the right femur, L3-L4 vertebral bodies, and L5-L6 cancellous cores. pQCT scan settings and analysis parameters are provided in Supplemental Table S1. Ex vivo pQCT and DXA data for L3 and L4 bodies were averaged, as were L5 and L6 cancellous core data.

Terminal ex vivo micro-CT was performed with a high-resolution Micro-CT system (Scanco Medical AG micro-CT 100) and 3-D morphometry evaluation program (software version uCT V6.1). The 12th thoracic vertebral body (T12), distal femur, and L6 cancellous cores were scanned at a 34-μm voxel resolution. Humeral beams (described below) were scanned at 5-μm resolution. Supplemental Table S2 provides settings for micro-CT analyses.

Bone biomechanics

Bone samples collected after 16 months of treatment were trimmed and scanned by DXA, pQCT, and/or micro-CT prior to destructive biomechanical testing. L3 and L4 bodies were dissected, leaving parallel-cut caudal and cranial surfaces with exposed trabecular bone. Cylindrical cancellous cores (~ 5 mm diameter) were prepared from the middle region of similarly prepared L5 and L6 bodies. The cores were harvested in the caudal-cranial plane, and each core was then bisected into caudal and cranial halves of approximately 4 mm in height. Trimmed L3 and L4 bodies as well as L5 and L6 cancellous cores, the femoral diaphysis, and the femoral neck were tested using an MTS 858 Mini Bionix Servohydraulic Test System, Model 358.02C. Data were collected using TestSuite TWE version 3.1.2. Cortical beams (1 by 3 by 35 mm) milled from the caudal aspect of the right humeral diaphysis were tested in three-point bending (Bose ElectroForce® 3300 system, WinTest® 4.1). Destructive tests of the right femur (3-point bending), femoral neck (shear test, simulated single-legged stance), vertebral specimens (compression), and humeral beams were conducted and data were calculated as previously described [22], with the following variations: the L3-L4 tests used a 0.5% offset for yield load, and the L5-L6 core tests used a 0.5% offset for yield load and a 2% offset for peak load, stiffness, and work to failure (energy, i.e., area under the load-displacement curve, AUC). L3 and L4 biomechanics data were averaged, as were L5 and L6 cancellous core biomechanics data.

Estimated femoral diaphyseal material properties included ultimate stress ($FLc/4I$; F = peak load, L = span length, c = radius, and I = cross-sectional moment of inertia), modulus ($SL3/48I$; S = stiffness), and toughness ($0.75 \times \text{AUC} \times b2 / LI$; b = diameter). Apparent material properties calculated for L3-L4 bodies and L5-L6 cores included apparent strength (peak load/area), apparent modulus ([stiffness × height] / area), and apparent toughness (AUC / [area × height]).

Statistics

For biochemistry, bone turnover markers, and densitometry data, homogeneity of group variances was assessed by Levene's test. Datasets with nonsignificant Levene's test were evaluated by one-way homoscedastic ANOVA. For datasets with significance by Levene's test, a heteroscedastic ANOVA was used. ANOVAs with a significant F test were followed by Dunnett's test comparing each group to the Veh control group. Correlations between bone mass and strength were first assessed via multivariate tests of regression line equality. If significant group effects for regression line slopes or intercepts were observed, Pearson's correlation test was applied to evaluate each group versus Veh controls. If no group differences were determined, Pearson's correlation test was applied on all groups combined. Statistics were performed using SAS system for Windows, Version V8.2 and V9.2.

Results

General health and clinical observations

The success of OVX surgery was confirmed by lack of ovaries at necropsy, reduced uterus weight, and lower serum estradiol compared with sham controls (data not shown). One sham group animal was excluded based on uterine atrophy at necropsy suggesting natural menopause, and another sham animal was euthanized at week 55 due to poor and deteriorating health, potentially related to kidney disease. One Veh animal developed diabetes and died at week 50. One animal from the ABL0.2 group was euthanized on day 7 of treatment due to poor and deteriorating health that was evident during the pretreatment period. There were no clinical observations related to abaloparatide and no abaloparatide-related changes in food consumption or body weight. Abaloparatide had no adverse effects on gross pathology, organ weights, or histopathology or on clinical chemistry, coagulation, hematology, or urinalysis parameters (data not shown). Radiographic assessments indicated no abaloparatide-related abnormalities that might indicate localized proliferative changes (data not shown).

Clinical chemistry

Abaloparatide had no significant effects on serum levels of calcium, phosphorus, endogenous PTH, $1,25(OH)_2D$, or creatinine (Supplemental Table S3) compared with Veh controls.

Biochemical markers of bone turnover

The bone formation markers serum P1NP and BSAP were significantly higher in Veh versus sham controls at all post-OVX time points, as were the resorption markers serum CTX and urine NTX, consistent with OVX-induced increases in bone remodeling (Supplemental Table S4). Abaloparatide led to greater serum P1NP levels relative to Veh controls, with effects reaching statistical significance at months 3, 7.5, and 12 for the 0.2-μg/kg dose, whereas the two higher doses did not show significance. There were no statistically significant effects of abaloparatide on serum BSAP, serum CTX, or urine NTX at any time point (Supplemental Table S4).

Bone histomorphometry

After 25 total months of OVX, including 16 months of treatment, most histomorphometry endpoints for L2, femoral neck, and femoral diaphysis showed no significant differences among groups (Fig. 1 and Supplemental Tables S5, S6, and

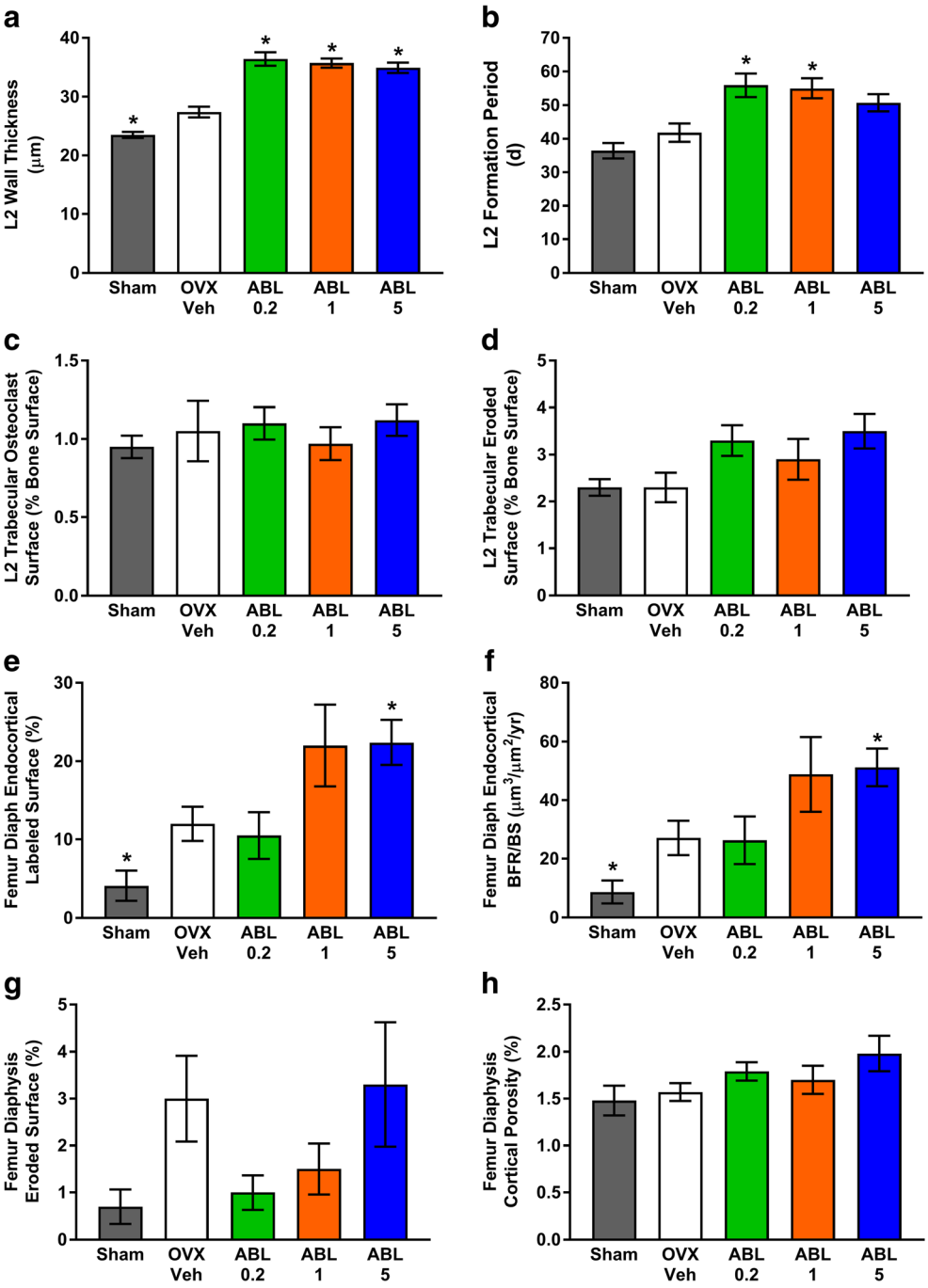

Fig. 1 Histomorphometry for L2 vertebra trabecular bone (**a**–**d**) and femoral diaphysis cortical bone (**e**–**h**) in the 16-month study. Data were obtained after 16 months of treatment and are presented as means ± SEM, n = 14–16/group. *$P < 0.05$ versus Veh controls

S7). L2 showed significantly greater trabecular osteoblast surface per bone surface (Tb.Ob.S/BS) and mineralizing surface per bone surface (Tb.MS/BS) in Veh versus sham controls, consistent with OVX-induced increases in bone remodeling (Supplemental Table S5). L2 wall thickness (W.Th) was significantly higher in Veh versus sham controls, and L2 W.Th was significantly higher in all abaloparatide groups versus Veh (Fig. 1a). L2 formation period (FP) was significantly higher in the ABL0.2 and ABL1 groups versus Veh controls (Fig. 1b), driven by increased W.Th without an increase in adjusted apposition rate (Aj.AR) (Supplemental Table S5). L2 osteoclast surface per bone surface (Oc.S/BS) and eroded surface per bone surface (ES/BS) were similar in each abaloparatide group versus Veh controls (Fig. 1c, d).

Trabecular bone parameters at the femoral neck showed few significant differences between groups. Ob.S/BS and W.Th were significantly greater in Veh versus sham controls, and the ABL1 group had significantly greater single-labeled surface per bone surface (sLS/BS) ($P < 0.05$ versus Veh controls; Supplemental Table S6). Femoral neck Oc.S/BS, ES/BS, and bone formation rate per bone surface (BFR/BS) were similar in abaloparatide versus Veh groups (Supplemental Table S6).

Cortical histomorphometry at the femoral diaphysis indicated that single and/or double Haversian fluorochrome labels were evident in every animal from each group. Likewise, single and/or double endocortical and periosteal labels were evident in all animals in the ABL1 and ABL5 groups. No single or double endocortical labels were observed for seven Sham animals, one Veh animal, and two ABL0.2 animals, and no periosteal labels were observed in seven Sham animals, one Veh animal, and one ABL0.2 animal; for these cases, a mineral apposition rate (MAR) value of 0.2 μm/day was imputed. Significantly greater endocortical labeled surface and endocortical BFR/BS was observed in the femoral diaphysis of Veh controls versus sham controls (Fig. 1e, f). The femoral diaphysis of Veh controls also showed significantly greater Haversian labeled surface (H.L.Pm/H.Pm), higher MAR (H.MAR), and higher BFR (H.BFR/BS) versus sham controls (Supplemental Table S7). The ABL5 group had significantly greater femoral diaphysis endocortical labeled surface and higher endocortical BFR/BS compared with the Veh group (Fig. 1e, f). The abaloparatide groups showed no differences in the resorption parameters endocortical eroded surface or cortical porosity compared with Veh controls (Fig. 1g, h).

In vivo DXA

In vivo DXA of the whole body and specific axial and appendicular sites indicated that animals from the four combined OVX groups lost significant BMD between the start (month − 9) and end (month 0) of the bone depletion period, as compared with sham controls (Fig. 2). Similar trends in BMD were observed in Sham animals and Veh controls during the treatment period. The ABL1 and ABL5 groups showed significantly greater increases in whole body aBMD, starting as early as treatment month 4 ($P < 0.05$ versus Veh; Fig. 2a). Each abaloparatide dose significantly increased L1-4 aBMD as early as treatment month 4 ($P < 0.05$ versus Veh; Fig. 2b). The ABL5 group showed significantly increased cortical aBMC in the proximal tibia at month 16 (Fig. 2c). aBMD of the proximal femur, femoral neck, and trochanter was significantly increased in the ABL1 and ABL5 groups ($P < 0.05$ versus Veh; Fig. 2d–f).

pQCT

pQCT indicated that animals from the four combined OVX groups experienced significant bone loss at the proximal tibia during the bone depletion period, as compared with sham controls (Fig. 3). The Veh group exhibited some recovery of tibial bone loss during the treatment period (Fig. 3a–c, g–h). Abaloparatide at 1 and 5 μg/kg fully reversed OVX-induced deficits in proximal tibial total volumetric BMC (vBMC) and vBMD (Fig. 3a, b). All abaloparatide doses also caused significant gains in the cortical/subcortical compartment, including increased cortical/subcortical area and BMD (Fig. 3c, d). pQCT of the proximal tibial diaphysis revealed significant cortical bone gains with abaloparatide: Abaloparatide at 5 μg/kg increased endocortical bone apposition, as shown by significantly lower endocortical circumference versus Veh controls (Fig. 3e), and abaloparatide at 5 μg/kg also increased cortical thickness and vBMC ($P < 0.05$ versus Veh; Fig. 3g, h). Abaloparatide did not influence cortical vBMD of the proximal tibial diaphysis or the distal radial diaphysis at month 16 (Supplemental Table S8), nor did abaloparatide influence the percentage change in cortical vBMD from month 0 to month 16 at these sites (data not shown). Ex vivo pQCT analyses also suggested that abaloparatide had no significant effects on cortical vBMD of the femoral diaphysis (Supplemental Table S8).

Micro-CT

Month 16 micro-CT of the distal femoral metaphysis and the T12 cortical shell indicated lower cortical vBMD in Veh versus sham controls, whereas cortical vBMD in the three abaloparatide groups was similar to Veh controls (Supplemental Table S8). Cortical vBMD of humeral beams was also similar in the abaloparatide and Veh groups (Table S8), as was cortical porosity. Humeral beam cortical porosity as a percentage of cortical volume was 2.30 ± 0.27 (mean ± SEM) for the Sham group, 3.75 ± 0.42 for the Veh group ($P < 0.05$ versus Sham), 3.85 ± 0.42 for the ABL0.2 group (NS versus Veh), 3.45 ± 0.22 for the ABL1 group (NS versus Veh), and 3.54 ± 0.40 for the ABL5 group (NS versus Veh). Micro-CT of L6 cancellous cores showed lower vBMC and lower bone volume per total volume (BV/TV) in Veh versus sham controls, while the ABL1 and ABL5 groups had greater vBMC and BV/TV compared with Veh (Fig. 4a, b). Abaloparatide also dose-dependently reversed the deleterious OVX-related increase in L6 structural model index (SMI) (Fig. 4c). Representative micro-CT reconstructions of L6 cores for the OVX-Veh and ABL1 groups (Fig. 4d) also depict the denser and more robust trabecular architecture associated with abaloparatide administration.

Bone biomechanics

There were no significant differences between the Veh and other groups for biomechanical parameters of the femoral diaphysis, femoral neck, and humeral beams (Supplemental Tables S9–11). Peak and yield load values for L3-L4 vertebral bodies and L5-L6 cancellous cores were significantly lower in Veh versus sham controls (Fig. 5a–d). The Veh group also had significantly lower values for L3-L4 energy (Supplemental Table S12) and L5-L6 core stiffness (Fig. 5e) compared with sham controls, whereas these parameters were similar in the abaloparatide and Veh groups. The ABL5 group had

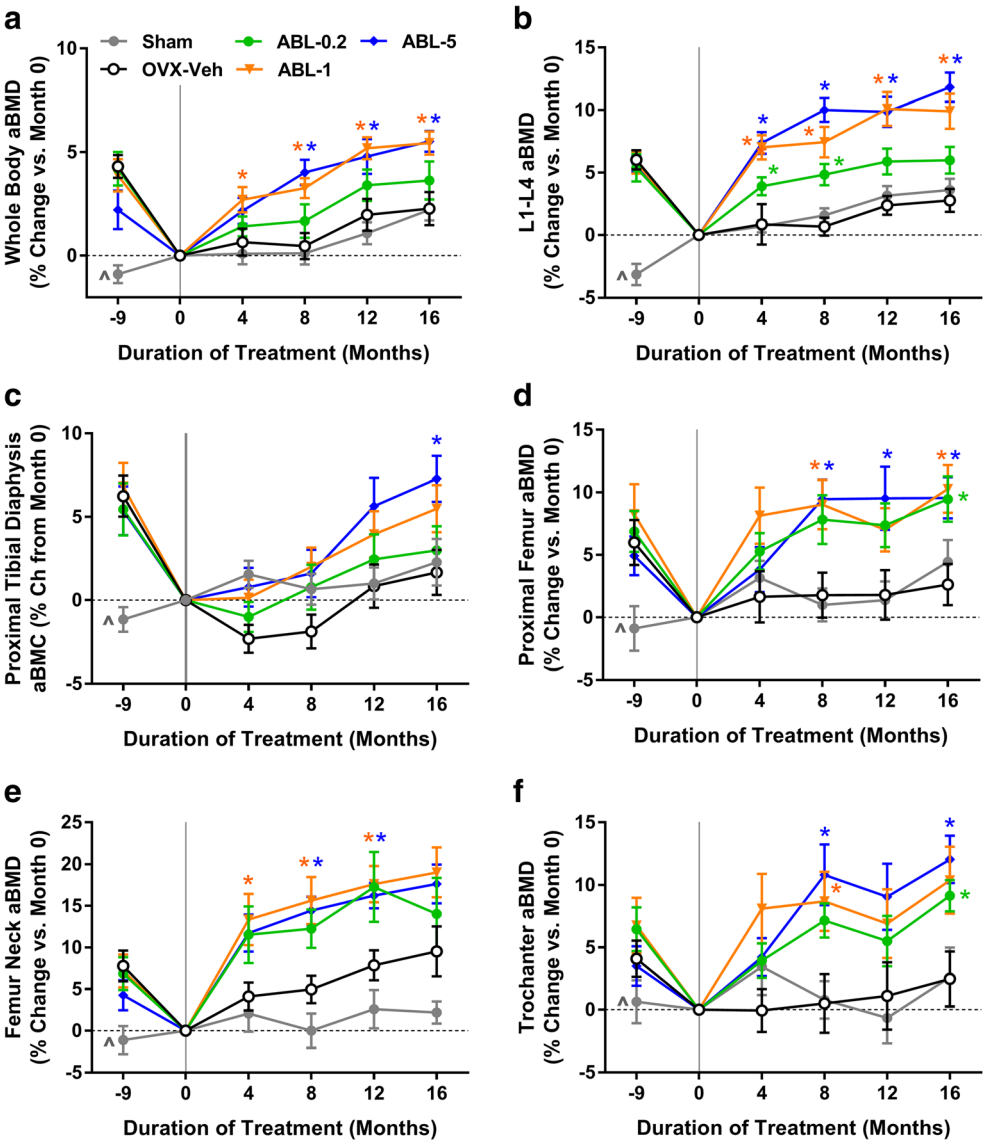

Fig. 2 Changes in aBMD by in vivo DXA in 16-month study. Month − 9 represents the time of sham or OVX surgery, and month 0 marks the beginning of treatment. Data represent means ± SEM, $n = 14–16$/group. *$P < 0.05$ versus Veh control group. ^$P < 0.05$ for sham controls versus the four combined OVX groups at month − 9

significantly greater L3-L4 peak load, and the ABL1 and ABL5 groups had significantly greater L5-L6 cancellous core peak load, yield load, stiffness, and energy (all $P < 0.05$ versus Veh; Fig. 5). Linear regression analyses were performed to assess relationships between bone mass and bone strength, which are considered to represent measures of bone quality. Significant positive relationships were observed for L3-L4 peak load versus QCT-derived total vBMC for all five groups, with r^2 values ranging from 0.55 to 0.83. For these regressions, slopes were significantly steeper for the sham, ABL1, and ABL5 groups versus Veh controls, indicating greater L3-L4 strength than might be expected from bone mass (Fig. 5g). For all other bone mass-strength relationships, similar regression lines were observed for each of the five groups, which enabled calculations of overall r^2 values for all groups combined. L5-L6 core peak load correlated positively with ex vivo QCT vBMC (Fig. 5h), with an overall r^2 of 0.87 ($P < 0.05$). Femoral shaft peak load correlated positively with femoral shaft cortical vBMC, with an overall r^2 of 0.85, and femoral neck peak load correlated positively with femoral neck aBMC, with an overall r^2 of 0.54 (both $P < 0.05$) (Fig. 6).

Discussion

This study demonstrated that abaloparatide, a selective PTH1 receptor agonist, stimulated bone formation and increased bone mass in osteopenic OVX cynos relative to Veh controls. After 16 months of treatment, vertebral bone strength was significantly higher in the two highest-dose abaloparatide groups versus Veh controls, while the strength of cortical beams was similar in the abaloparatide groups and the Veh controls. Relationships between bone mass and strength were maintained or enhanced by

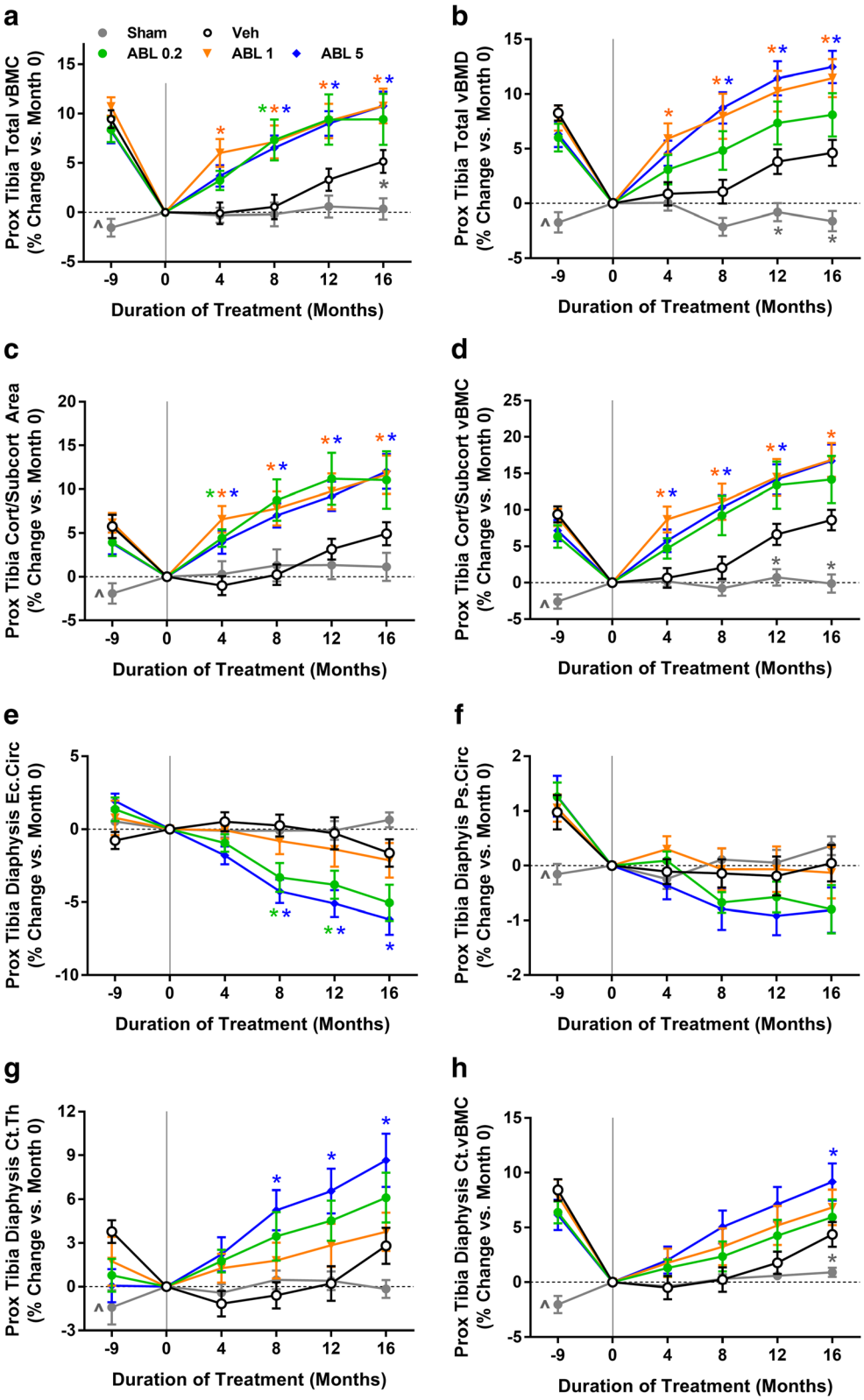

Fig. 3 Changes in pQCT parameters at the proximal tibia in 16-month study. Month −9 reflects the time of sham or OVX surgery, and month 0 reflects the beginning of the 16-month treatment period. Data represent means ± SEM, $n = 14–16$/group. *$P < 0.05$ versus Veh control group. ^$P < 0.05$ for sham controls versus the four combined OVX groups at month −9

abaloparatide across all doses, indicating preserved or improved bone quality. Abaloparatide did not increase serum calcium, bone resorption parameters, or cortical porosity and did not reduce cortical BMD, which is a potentially novel set of findings in nonhuman primates receiving long-term daily s.c. administration of PTHR1 agonists.

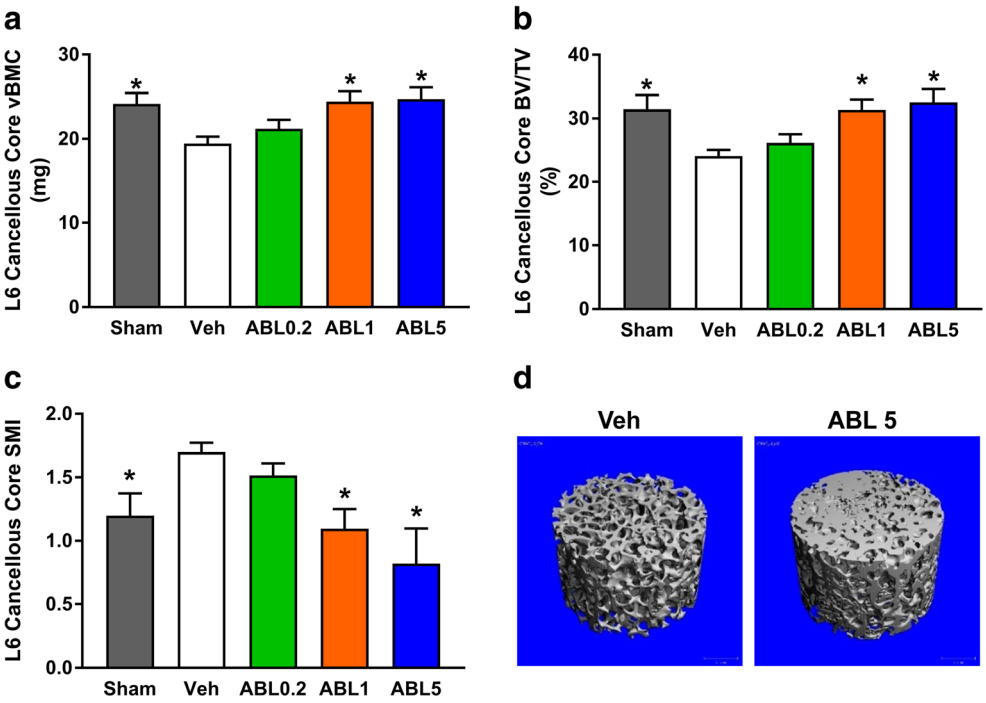

Fig. 4 Micro-CT results for L6 cancellous cores in 16-month study. **a** Volumetric BMC (vBMC). **b** Bone volume per total volume (BV/TV). **c** Structural model index (SMI). Data represent means ± SEM, $n = 14–16$/group. $^*P < 0.05$ versus Veh controls. **d** Micro-CT reconstructions of L6 cancellous cores for the Veh group and the ABL5 group, based on samples with vBMC and BV/TV values closest to their group's median values

pQCT and DXA indicated abaloparatide increased bone mass and density at cortical and trabecular sites. Abaloparatide administration was associated with significantly higher trabecular bone volume and strength in L6 cancellous cores, suggesting responsiveness of cancellous bone to abaloparatide anabolism. Higher endocortical bone formation in the femur and QCT-based evidence for bone apposition at the endocortical surface of the femur suggest that long bone endocortices also respond anabolically to abaloparatide. Higher L2 wall thickness in abaloparatide-treated animals suggests that abaloparatide may promote the over-filling of resorption spaces, which could contribute to treatment-related gains in bone volume and BMD. There was no evidence in this study for abaloparatide-related increases in bone resorption, with the abaloparatide groups and Veh controls exhibiting similar values for trabecular eroded surface and osteoclast surface in L2 and the femoral neck, similar endocortical eroded surface in the femoral diaphysis, and no differences in cortical porosity or biochemical markers of bone resorption.

The lack of observed effects of abaloparatide on cortical porosity and other bone resorption parameters in these cynos is consistent with OVX rat data showing no increases in bone resorption parameters with high doses of abaloparatide over a 12-month treatment period [5]. Such findings may be noteworthy because intermittent PTH therapy with full-length PTH or teriparatide was shown to increase bone resorption in OVX rats [23] and in nonhuman primates [10, 11]. Increased bone resorption with intermittent PTH or teriparatide therapy can be associated with transient hypercalcemia [7, 13, 24, 25], and the current studies showed no effects of abaloparatide on serum calcium, similar to previous findings from abaloparatide-treated cynos [18]. A study in postmenopausal women with osteoporosis showed that abaloparatide transiently increased serum calcium and increased bone resorption markers, though these responses were less pronounced compared with the active comparator teriparatide [2, 3]. Teriparatide was previously shown to increase serum $1,25(OH)_2D$ and suppressed endogenous PTH in OVX cynos [26], and such responses were not observed with abaloparatide treatment in this OVX cyno study.

Increased bone resorption with intermittent PTH can increase cortical porosity [7–11] and endocortical bone resorption [9, 10], which may explain PTH-induced reductions in cortical BMD observed in preclinical [9–11] and clinical studies [12, 13]. In the current study, abaloparatide had no apparent effects on endocortical eroded surface at the femoral diaphysis or on cortical porosity of the femoral or humeral diaphysis. The lack of increased porosity may explain why abaloparatide did not reduce cortical vBMD at any of six sites analyzed. Recent clinical data from iliac crest bone biopsies showed significantly greater cortical porosity in postmenopausal women treated with abaloparatide or teriparatide compared with placebo controls [27]. Those iliac crest analyses also showed that the abaloparatide group (but not the teriparatide group) had significantly lower trabecular eroded surface values compared with placebo, a difference that was not observed in the current OVX cyno study. Reasons for these apparent discrepancies may relate to differences in species, the nature of estrogen deficiency (OVX in cynos versus natural menopause in human subjects), and/or to differences in the anatomical sites for bone histomorphometry analyses.

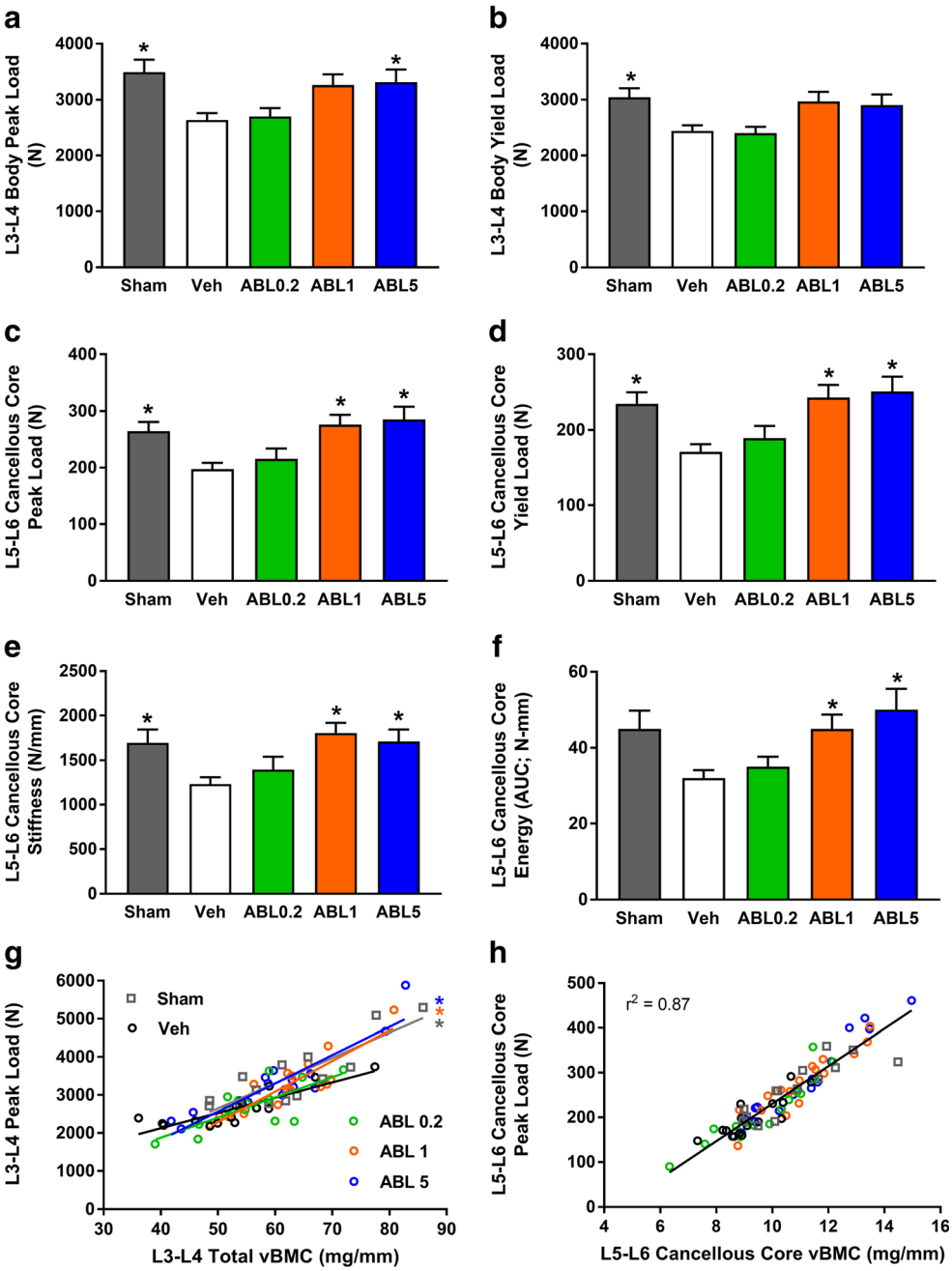

Fig. 5 **a**–**f** Destructive biomechanical testing data for L3-L4 vertebral bodies and L5-L6 cancellous cores in 16-month study. Data represent means ± SEM, $n = 14$–16/group. *$P < 0.05$ versus Veh controls. **g** Linear regressions for L3-L4 vertebral body peak load versus vBMC; r^2 values were Sham = 0.73, Veh = 0.75, ABL0.2 = 0.55, ABL1 = 0.79, ABL5 = 0.83 (all $P < 0.05$). *Asterisk*: Regression lines for the Sham, ABL1, and ABL5 groups had significantly steeper slopes than Veh controls ($P < 0.05$). H. L5-L6 core peak load versus vBMC; r^2 value represent all groups combined, $P < 0.05$

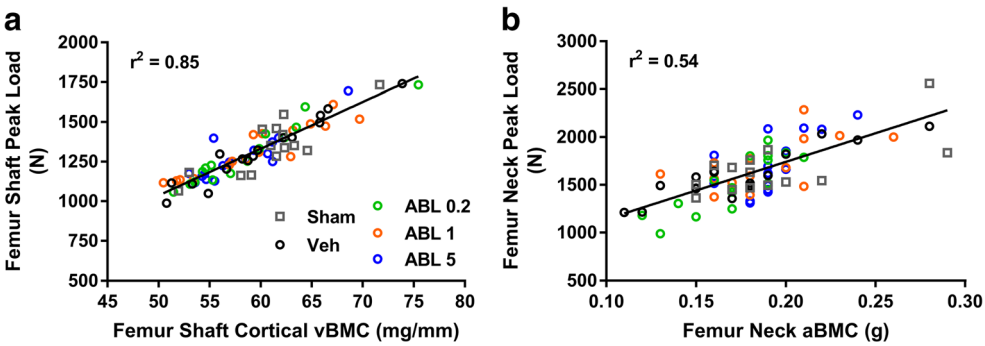

Fig. 6 Linear regressions for **a** femoral shaft peak load versus ex vivo vBMC and **b** femoral neck peak load versus in vivo (terminal) femoral neck aBMC. r^2 values represent all groups combined. Both r^2 values were significant ($P < 0.05$)

While the abaloparatide groups from this cyno study showed no evidence of increased cortical porosity or reduced cortical vBMD, they nonetheless exhibited increased endocortical bone formation, reduced endocortical circumference, and increased cortical thickness. These findings suggest that increased bone formation with abaloparatide can improve cortical geometry without concomitant intracortical bone loss, which may represent a desirable pharmacodynamic profile. It has been a long-standing clinical goal to minimize the pro-resorptive effects of intermittent PTH therapy while maintaining its anabolic (bone-forming) effects, which has the potential to magnify BMD gains. Some [12, 28] but not all clinical investigational approaches [29, 30] delivered on this goal by co-administering an antiresorptive agent. Abaloparatide as a monotherapy appears capable of increasing bone formation with limited effects on resorption, which may have favorable implications for improving bone mass and strength. Mechanistically, studies with cultured bone cells showed that abaloparatide caused less sustained increases in pro-resorptive cytokines compared with teriparatide, whereas both agents caused similar changes in factors that regulate bone formation [31].

The main purpose of the current study was to assess the effects of abaloparatide on bone strength and bone quality. The abaloparatide 1 and 5 μg/kg groups exhibited significantly greater lumbar vertebral strength versus Veh controls, which can be largely explained by increased vertebral bone mass and volume. Teriparatide and PTH(1–84) have also been shown to increase vertebral strength in OVX monkeys [32, 33]. Similar to previous findings in OVX cynos treated with teriparatide [8], abaloparatide had no significant effects on long bone bending strength, whereas PTH(1–84) reduced several long bone bending strength parameters in OVX rhesus monkeys [9]. Abaloparatide had no significant effects on femoral neck strength, similar to previous findings with PTH(1–84) in OVX rhesus monkeys [10]. Teriparatide was previously shown to increase femoral neck strength when administered for 18 months to acutely ovariectomized (nonosteopenic) cynos [11], whereas in the current study, abaloparatide administration was delayed until the femoral neck had established osteopenia and lasted for 16 months.

An important bone quality finding was that abaloparatide administration maintained biomechanical properties of prismatic humeral beams and also maintained the estimated material properties of the femoral diaphysis. Those findings indicate that abaloparatide had no untoward effects on bone material properties at these sites. Bone quality was also assessed by analyzing bone mass-strength relationships, which are usually positive and linear in the absence of treatment [6, 22]. Treatments that impair matrix quality can create biomechanically unfavorable shifts in bone mass-strength relationships [6, 34]. Abaloparatide maintained positive linear relationships between bone mass and strength at all sites examined, including the vertebrae, femoral diaphysis, and femoral neck. For L3-L4 vertebrae, abaloparatide caused a biomechanically favorable shift in the relationship between BMC and peak load, with a steeper slope indicating greater strength than would be predicted by the bone mass. Explanations for this shift are unclear and could relate in part to improved trabecular architecture; micro-CT of L6 cancellous cores showed that abaloparatide significantly reduced SMI, indicating a shift towards more robust plate-like trabecular architecture. SMI is associated with vertebral strength [35], and this relationship is partially independent of BMD [36], suggesting improved SMI may indicate an improvement in bone quality.

Strengths of this study include wide ranges of abaloparatide doses, longitudinal assessments of bone mass and geometry at sites prone to fracture in humans, micro-CT-based analyses of microarchitecture and porosity, and a prolonged post-OVX bone depletion period that allowed significant cortical and trabecular bone deterioration prior to treatment initiation. Study limitations include the absence of interim histomorphometry that may have identified earlier effects of OVX and/or abaloparatide, including possible increases in bone formation or bone resorption that were no longer evident at necropsy. Indeed, a previous OVX cyno study showed that interim iliac crest biopsy samples collected after 6 months of abaloparatide treatment exhibited higher trabecular bone formation compared with Veh controls, whereas bone resorption parameters were similar between the groups [16]. An active comparator such as teriparatide would also have been helpful for understanding pharmacodynamic differences between teriparatide and abaloparatide, though some insights may be revealed over time based on recent clinical trials comparing the two agents [2, 3]. Finally, several abaloparatide-related findings described in the current preclinical report appear to differ from those observed in the pivotal abaloparatide phase 3 fracture trial [3, 27]; these differences include certain cortical porosity and eroded surface findings, as mentioned above, as well as the observation that abaloparatide did not significantly increase long bone strength in the OVX cynos, whereas abaloparatide significantly reduced nonvertebral fractures clinically [3].

In summary, abaloparatide administration was associated with significantly greater bone formation, bone volume, bone density, and bone strength in osteopenic OVX cynos while having no apparent effects on bone resorption parameters. Bone quality was preserved at purely cortical sites and was maintained or improved at trabecular-rich sites such as the femoral neck and vertebrae. These findings are consistent with evidence of reduced fracture risk with abaloparatide in postmenopausal women with osteoporosis [3], while also suggesting that gains in BMD in abaloparatide-treated patients reflect site-specific improvements in bone strength.

Acknowledgements This study was supported by Radius Health. The authors acknowledge the important technical and scientific contributions of Roger O'Reilly, Sabile Fityani-Trimm, Farideh Nourian, Thomas Greutzner, Nacéra Mellal, and the Biomarker, Imaging, and Histomorphometry Technical Teams all from Charles River Laboratories, Senneville, Quebec.

Paul Kostenuik, PhD (Phylon Pharma Services) provided medical writing assistance with support from Radius Health.

Compliance with ethical standards

Conflicts of interest MSO and GH are employees at Radius Health, Inc.

References

1. Culler MD, Dong J, Shen Y et al (2001) BIM-44058, a novel analog of PTHrP with enhanced bone building activity, but decreased calcium-mobilization potential. J Bone Miner Res 16:S540
2. Leder BZ, O'Dea LS, Zanchetta JR, Kumar P, Banks K, McKay K, Lyttle CR, Hattersley G (2015) Effects of abaloparatide, a human parathyroid hormone-related peptide analog, on bone mineral density in postmenopausal women with osteoporosis. J Clin Endocrinol Metab 100(2):697–706. https://doi.org/10.1210/jc.2014-3718
3. Miller PD, Hattersley G, Riis BJ, Williams GC, Lau E, Russo l, Alexandersen P, Zerbini CAF, Hu M, Harris AG, Fitzpatrick l, Cosman F, Christiansen C, for the ACTIVE Study Investigators (2016) Effect of abaloparatide vs placebo on new vertebral fractures in postmenopausal women with osteoporosis: a randomized clinical trial. JAMA 316(7):722–733. https://doi.org/10.1001/jama.2016.11136
4. Varela A, Chouinard L, Lesage E, Smith SY, Hattersley G (2017) One year of abaloparatide, a selective activator of the PTH1 receptor, increased bone formation and bone mass in osteopenic ovariectomized rats without increasing bone resorption. J Bone Miner Res 32(1):24–33. https://doi.org/10.1002/jbmr.3003
5. Varela A, Chouinard L, Lesage E, Guldberg R, Smith SY, Kostenuik PJ, Hattersley G (2017) One year of abaloparatide, a selective peptide activator of the PTH1 receptor, increased bone mass and strength in ovariectomized rats. Bone 95:143–150. https://doi.org/10.1016/j.bone.2016.11.027
6. Hernandez CJ, Keaveny TM (2006) A biomechanical perspective on bone quality. Bone 39(6):1173–1181. https://doi.org/10.1016/j.bone.2006.06.001
7. Boyce R, Paddock C, Franks A, Jankowsky M, Eriksen E (1996) Effects of intermittent hPTH(1-34) alone and in combination with $1,25(OH)_2D_3$ or risedronate on endosteal bone remodeling in canine cancellous and cortical bone. J Bone Miner Res 11(5):600–613. https://doi.org/10.1002/jbmr.5650110508
8. Burr D, Hirano T, Turner C, Hotchkiss C, Brommage R, Hock J (2001) Intermittently administered human parathyroid hormone (1-34) treatment increases intracortical bone turnover and porosity without reducing bone strength in the humerus of ovariectomized cynomolgus monkeys. J Bone Miner Res 16(1):157–165. https://doi.org/10.1359/jbmr.2001.16.1.157
9. Fox J, Miller MA, Newman MK, Recker RR, Turner CH, Smith SY (2007) Effects of daily treatment with parathyroid hormone 1-84 for 16 months on density, architecture and biomechanical properties of cortical bone in adult ovariectomized rhesus monkeys. Bone 41(3):321–330. https://doi.org/10.1016/j.bone.2007.04.197
10. Fox J, Miller MA, Recker RR, Turner CH, Smith SY (2007) Effects of treatment of ovariectomized adult rhesus monkeys with parathyroid hormone 1-84 for 16 months on trabecular and cortical bone structure and biomechanical properties of the proximal femur. Calcif Tissue Int 81(1):53–63. https://doi.org/10.1007/s00223-007-9036-y
11. Sato M, Westmore M, Ma Y, Schmidt A, Zeng Q, Glass E, Vahle J, Brommage R, Jerome C, Turner C (2004) Teriparatide [PTH-(1-34)] strengthens the proximal femur of ovariectomized nonhuman primates despite increasing porosity. J Bone Miner Res 19(4):623–629. https://doi.org/10.1359/JBMR.040112
12. Tsai JN, Uihlein AV, Lee H, Kumbhani R, Siwila-Sackman E, McKay EA, Burnett-Bowie S-AM, Neer RM, Leder BZ (2013) Teriparatide and denosumab, alone or combined, in women with postmenopausal osteoporosis: the DATA study randomised trial. Lancet 382(9886):50–56. https://doi.org/10.1016/S0140-6736(13)60856-9
13. Neer R, Arnaud C, Zanchetta J et al (2001) Effect of parathyroid hormone (1-34) on fractures and bone mineral density in postmenopausal women with osteoporosis. N Engl J Med 344(19):1434–1441. https://doi.org/10.1056/NEJM200105103441904
14. Smith SY, Jolette J, Turner CH (2009) Skeletal health: primate model of postmenopausal osteoporosis. Am J Primatol 71(9):752–765. https://doi.org/10.1002/ajp.20715
15. Kostenuik PJ, Smith SY, Jolette J, Schroeder J, Pyrah I, Ominsky MS (2011) Decreased bone remodeling and porosity are associated with improved bone strength in ovariectomized cynomolgus monkeys treated with denosumab, a fully human RANKL antibody. Bone 49(2):151–161. https://doi.org/10.1016/j.bone.2011.03.769
16. Legrand J, Becret A, Fisch C, Attia M, De Jouffrey S, Dong JZ, Woon CW, Claude CJ, Cullen MD (2001) BIM-44058, a novel PTHrP analog, increases bone formation but not bone resorption histomorphometric parameters in old ovariectomized cynomolgus monkeys. J Bone Miner Res 16:S539
17. Legrand J, Fisch C, Guillaumat P, De Jouffrey S, Dong JZ, Woon CW, Claude J, Culler MD (2001) BIM-44058, a novel PTHrP analog, restores in vivo spinal bone mineral density in old ovariectomized osteopenic cynomolgus monkeys. J Bone Miner Res 16:S539
18. Legrand J, Guillaumat P, Forster R, Dong JZ, Woon CW, Claude J, Culler MD (2001) BIM-44058, a novel PTHrP analog, does not increase total plasma calcium in cynomolgus monkeys at an effective pharmacological dose. J Bone Miner Res 16:S539
19. CHMP (2005) Guideline on the evaluation of new medicinal products in the treatment of primary osteoporosis. European Medicines Agency, Rev 2 http://www.ema.europa.eu/docs/en_GB/document_library/Scientific_guideline/2009/09/WC500003406.pdf
20. FDA (1994) FDA draft guidelines for preclinical and clinical evaluation of agents used in the prevention or treatment of postmenopausal osteoporosis. http://www.fda.gov/downloads/ScienceResearch/SpecialTopics/WomensHealthResearch/UCM131206.pdf
21. Parfitt AM, Drezner MK, Glorieux FH, Kanis JA, Malluche H, Meunier PJ, Ott SM, Recker RR (1987) Bone histomorphometry: standardization of nomenclature, symbols, and units. Report of the ASBMR Histomorphometry Nomenclature Committee. J Bone Miner Res 2(6):595–610. https://doi.org/10.1002/jbmr.5650020617
22. Ominsky MS, Stouch B, Schroeder J, Pyrah I, Stolina M, Smith SY, Kostenuik PJ (2011) Denosumab, a fully human RANKL antibody, reduced bone turnover markers and increased trabecular and

cortical bone mass, density, and strength in ovariectomized cynomolgus monkeys. Bone 49(2):162–173. https://doi.org/10.1016/j.bone.2011.04.001

23. Kostenuik P, Capparelli C, Morony S, Adamu S, Shimamoto G, Shen V, Lacey D, Dunstan C (2001) OPG and PTH-(1-34) have additive effects on bone density and mechanical strength in osteopenic ovariectomized rats. Endocrinology 142(10):4295–4305. https://doi.org/10.1210/endo.142.10.8437
24. Body JJ, Gaich GA, Scheele WH, Kulkarni PM, Miller PD, Peretz A, Dore RK, Correa-Rotter R, Papaioannou A, Cumming DC, Hodsman AB (2002) A randomized double-blind trial to compare the efficacy of teriparatide [recombinant human parathyroid hormone (1-34)] with alendronate in postmenopausal women with osteoporosis. J Clin Endocrinol Metab 87(10):4528–4535. https://doi.org/10.1210/jc.2002-020334
25. Jerome C, Johnson C, Lees C (1995) Effect of treatment for 3 months with human parathyroid hormone 1-34 peptide in ovariectomized cynomolgus monkeys (Macaca fascicularis). Bone 17(4):415S–420S. https://doi.org/10.1016/8756-3282(95)00320-D
26. Brommage R, Hotchkiss CE, Lees CJ, Stancill MW, Hock JM, Jerome CP (1999) Daily treatment with human recombinant parathyroid hormone-(1-34), LY333334, for 1 year increases bone mass in ovariectomized monkeys. J Clin Endocrinol Metab 84(10):3757–3763. https://doi.org/10.1210/jcem.84.10.6039
27. Moreira CA, Fitzpatrick LA, Wang Y, Recker RR (2017) Effects of abaloparatide-SC (BA058) on bone histology and histomorphometry: the ACTIVE phase 3 trial. Bone 97:314–319. https://doi.org/10.1016/j.bone.2016.11.004
28. Leder BZ, Tsai JN, Uihlein AV, Burnett-Bowie SA, Zhu Y, Foley K, Lee H, Neer RM (2014) Two years of denosumab and teriparatide administration in postmenopausal women with osteoporosis (The DATA Extension Study): a randomized controlled trial. J Clin Endocrinol Metab 99(5):1694–1700. https://doi.org/10.1210/jc.2013-4440
29. Finkelstein JS, Hayes A, Hunzelman JL, Wyland JJ, Lee H, Neer RM (2003) The effects of parathyroid hormone, alendronate, or both in men with osteoporosis. N Engl J Med 349(13):1216–1226. https://doi.org/10.1056/NEJMoa035725
30. Black DM, Greenspan SL, Ensrud KE, Palermo L, McGowan JA, Lang TF, Garnero P, Bouxsein ML, Bilezikian JP, Rosen CJ (2003) The effects of parathyroid hormone and alendronate alone or in combination in postmenopausal osteoporosis. N Engl J Med 349(13):1207–1215. https://doi.org/10.1056/NEJMoa031975
31. Makino A, Takagi H, Sugiyama H, Kobayashi T, Kasahara Y (2015) Effects of abaloparatide on the expression of bone resorption- and formation-related factors in osteoblastic cells: a comparison with teriparatide. J Bone Miner Res 30:S369
32. Sato M, Westmore M, Clendenon J, Smith S, Hannum B, Zeng G, Brommage R, Turner C (2000) Three-dimensional modeling of the effects of parathyroid hormone on bone distribution in lumbar vertebrae of ovariectomized cynomolgus macaques. Osteoporos Int 11(10):871–880. https://doi.org/10.1007/s001980070047
33. Fox J, Miller MA, Newman MK, Turner CH, Recker RR, Smith SY (2007) Treatment of skeletally mature ovariectomized rhesus monkeys with PTH(1-84) for 16 months increases bone formation and density and improves trabecular architecture and biomechanical properties at the lumbar spine. J Bone Miner Res 22(2):260–273. https://doi.org/10.1359/jbmr.061101
34. Lafage M, Balena R, Battle M, Shea M, Seedor J, Klein H, Hayes W, Rodan G (1995) Comparison of alendronate and sodium fluoride effects on cancellous and cortical bone in minipigs. J Clin Invest 95(5):2127–2133. https://doi.org/10.1172/JCI117901
35. Fields AJ, Eswaran SK, Jekir MG, Keaveny TM (2009) Role of trabecular microarchitecture in whole-vertebral body biomechanical behavior. J Bone Miner Res 24(9):1523–1530. https://doi.org/10.1359/jbmr.090317
36. Ito M, Ikeda K, Nishiguchi M, Shindo H, Uetani M, Hosoi T, Orimo H (2005) Multi-detector row CT imaging of vertebral microstructure for evaluation of fracture risk. J Bone Miner Res 20(10):1828–1836. https://doi.org/10.1359/JBMR.050610